MAUSAM, **72**, 1 (January 2021), 215-228

551.515.2 : 551.509.313

Dynamics of Amphan Cyclone and associated changes in ocean, land meteorological and atmospheric parameters

AKSHANSHA CHAUHAN, RAMESH P. SINGH*, RAJESH KUMAR** and PRASANJIT DASH***

Center for Space and Remote Sensing Research, National Central University, Taiwan

**School of Life and Environmental Sciences, Schmid College of Science and Technology,*

Chapman University, Orange, USA

***Department of Environmental Science, Central University of Rajasthan, Ajmer, India*

****NOAA Center for Satellite Applications & Research,*

Colorado State Univ. CIRA, College Park, USA

e-mail : rsingh@chapman.edu

सार – बंगाल की खाड़ी और अंडमान सागर में मार्च-अक्टूबर के दौरान निम्न-दाब प्रणाली विकसित होने से अक्सर उष्णकटिबंधीय चक्रवात बनते हैं, भारतीय तटीय क्षेत्र के साथ भू-स्खलन वाले क्षेत्रों में तीव्रता के आधार पर व्यापक रूप से विनाश होता है। 20 मई, 2020 को दोपहर (भारतीय मानक समय 13.30 बजे) उष्ण कटिबंधीय चक्रवात अम्फन पश्चिम बंगाल के बख्खाली में भारतीय तट से टकराया। 19 मई, 2020 को इसकी तीव्रता 220 कि.मी./ घंटा पवन गति तक बढ़ कर एक महा चक्रवाती तूफान में बदल गई। इस चक्रवात से भारत और बांग्लादेश की एक बड़ी जनसंख्या प्रभावित हुई। 22 हज़ार से अधिक घर क्षतिग्रस्त हो गए, और लाखों व्यक्तियों को सुरक्षित स्थान पर स्थानांतरित किया गया तथा कोविड-19 के प्रसार के कारण, बचाव अभियान अत्यधिक चुनौतीपूर्ण था। चक्रवात का प्रभाव भारत के अधिकांश पूर्वी राज्यों पर पड़ा, चक्रवात के मार्ग पर भारी वर्षा हुई जिसके कारण बाढ़ आई। बहु-उपग्रह, ग्राउंड और अर्गो फ्लोट डेटा का उपयोग करते हुए, हमने मई 2020 के दौरान मौसम विज्ञानी और वायुमंडलीय प्राचलोंका विश्लेषण किया। हमारा विस्तृत विश्लेषण चक्रवात से पहले और बाद में वायुमंडलीय (CO मोल अंश, कुल ओजोन कॉलम) और महासागर प्राचलों (क्लोरोफिल सांद्रता, घुली हुई ऑक्सीजन, लवणता, समुद्री सतह और अधो-सतही तापमान) में स्पष्ट परिवर्तन दर्शाता है। जैसे जैसे चक्रवात भूमि पर आगे बढ़ता है वैसे वैसे महासागर के मापदंड, जैसे चक्रवात अम्फन के कारण उसके मार्ग में परिवर्तन तथा वायुमंडलीय और मौसम विज्ञानी प्राचल में परिवर्तन होता है।

ABSTRACT. The low-pressure system developed in the Bay of Bengal and the Andaman Sea during March-October, often forms tropical cyclones, depending upon the intensity widespread destruction occurs in the areas where landfall takes place along the Indian coastal region. On 20 May, 2020, tropical cyclone Amphan hit the Indian coast at Bakkhali, West Bengal, in the afternoon (1330 IST). On 19 May, 2020, the intensity strengthened into a super cyclonic storm, with a strong wind speed up to 220 km/h. This cyclone affected a large population of India and Bangladesh. More than twenty-two thousand houses were damaged and millions of people were shifted to a safe place and due to the spread of COVID-19, the rescue missions were quite challenging. The cyclone affected most of the eastern states of India, heavy rainfall occurred causing floods along the track of cyclones. Using multi-satellite, ground and Argo floats data, we have analyzed meteorological and atmospheric parameters during May 2020. Our detailed analysis shows pronounced changes in atmospheric (CO mole fraction, total ozone column) and ocean parameters (chlorophyll concentration, dissolved oxygen, salinity, sea surface and sub-surface temperature) before and after the cyclone. Changes in ocean parameters such as caused by the cyclone Amphan along its track and the atmospheric and meteorological parameters change as the cyclone moves over the land.

Key words – Amphan cyclone, Low pressure, Chlorophyll concentration, Argo floats, Super cyclone.

1. Introduction

The east coast of India is prone to tropical cyclones during pre and post-monsoon seasons, almost every year. Cyclones are developed over the Bay of Bengal and the Andaman Sea, known to be one of the most powerful atmospheric systems on the planet, playing a critical role in heat and energy transport, impacting mixed layer dynamics and aquatic ecosystems and having devastating effects on coastal populations (Roman-Stork and Subrahmanyam, 2020). Globally, there are annually over 80 tropical cyclones on average (Singh *et al.*, 2001; Frank and Roundy, 2006), with an average of 5 to 6 occurring in the Bay of Bengal, accounting for roughly 7% of global

tropical cyclones annually (Singh *et al.*, 2001). The movement of cyclones after its formation, towards land until landfall and afterward, cause large-scale destruction to life and properties over the coastal and inland regions (Chauhan *et al.*, 2018). The cyclone causes pronounced changes in the ocean, atmospheric, meteorological and land parameters which are now being monitored using multi satellites globally. The changes observed from satellite remote sensing data have shown a strong coupling between ocean-land-atmosphere-meteorological parameters associated with cyclone/hurricane (Hudhud, Fani and Harvey) (Gautam *et al.*, 2005a,b; Pathakoti *et al.*, 2016; Chauhan *et al.*, 2018, 2019, 2021; Sarkar *et al.*, 2018). A recent, study by Chauhan *et al*. (2021) using Argo floats data (ARGO project: https://argo.ucsd.edu/data/acknowledging-argo/) have shown pronounced changes in the vertical profile of salinity, temperature, dissolved oxygen (DO) with the movement of cyclone Fani along its track towards the north prior to its landfall.

Tropical cyclones cause large-scale destruction in the coastal region and region along their path (Chittibabu *et al.*, 2004; Powell and Reinhold, 2007; Turton and Stork, 2008; Chauhan *et al.*, 2018). The reason behind the high frequency of the tropical cyclone is the higher temperature from April to October which provides favorable conditions for tropical cyclone formation in the Indian subcontinent. Several major cyclones have formed in the Bay of Bengal (BoB) that impacted eastern coasts of India and devastated areas where the landfall occurred (Kundu *et al*., 2001; Mohapatra *et al.*, 2014; Pathakoti *et al.*, 2016; Chauhan *et al.*, 2018; Mohapatra and Sharma, 2019).

The southern parts of India are prone to cyclones during pre-monsoon and post-monsoon season. In a short span of nine months, two very severe cyclones, Titli and Fani, hit southern coasts and caused vast devastation (Mohanty *et al.*, 2019). In coastal regions, cyclones are responsible for large scale destruction due to storm surges and flooding in comparison to any other natural hazards every year (Mohapatra *et al.*, 2014; Mohapatra and Sharma, 2019; Rao *et al*., 2020) and affect weather conditions of a large region over India (Knutson *et al.*, 2010; Chauhan *et al.*, 2018). These cyclones affect both the coastal parts and much further inside the land (Kundu *et al.*, 2001; Chauhan *et al.*, 2018). The long coastline of India makes it more vulnerable to such complex weather systems. The storm water surges were caused by the cyclones and tsunami in the past which were responsible for the increase in the salinity of the freshwater ecosystems upstream through estuaries and creeks. This saline water intrusion leads to an impact on the physicochemical properties of the aqueous medium as well as ambient media. The increased salinity of the water has a harmful effect on the aquatic flora and fauna and modified the biodiversity of the region. Further, the surges associated with the cyclones and tsunami enhanced chlorophyll concentrations (Singh *et al*., 2007; Tang *et al.*, 2006, 2009).

During the cyclone, strong winds damage automatic weather stations deployed along with the coastal areas, under such conditions it is difficult to get any kind of meteorological data. However, numerous satellites from various international space agencies orbit the Earth which provides data about the land, ocean and atmospheric parameters. Satellite sounders can provide information about the meteorological and atmospheric parameters at different pressure levels. The multi-satellite remote sensing data are widely being used in all kinds of natural hazards applications, monitoring, damage mapping, early warning and study changes on the land, ocean, atmosphere and ionosphere (Singh, 2003). Kundu *et al.* (2001) used Indian Remote Sensing Satellite (IRS-P4) OCEANSAT satellite data which was launched on 26th May, 1999. The Indian OCEANSAT data were used to study the changes in the chlorophyll and suspended matter concentrations along the eastern coast of India hit by the 1999 super cyclone.

In this paper, detailed analysis of ocean (sea surface temperature, chlorophyll concentration, salinity, dissolved oxygen), meteorological and atmospheric parameters retrieved from satellite and Argo observations, which played an important role in the formation of the cyclone have been carried out. The detailed analysis of data shows strong changes in ocean ecology and stratospheric-tropospheric exchanges.

2. Cyclone Amphan

Among the natural calamities, the frequency of cyclones has increased having higher intensity in recent times which are the consequences of the changing climate. Cyclones are low-pressure systems formed over warm tropical waters, having a gale-force wind near the center. The winds spread hundreds of miles away from the center of the cyclone. The cyclonic storms are accompanied by large intensity rainfall and storm surges which results in flooding and a major loss of life and property. The grading of the tropical cyclones in the Bay of Bengal is based on the intensity of wind speeds at their center. The Bay of Bengal (BoB) represents the uppermost number of tropical cyclones worldwide, with the latest being Amphan cyclone (Mitra *et al.*, 2020). The cyclone often affects the east and west coasts of India (Kundu *et al.*, 2001; Evan *et al.*, 2011; Chauhan *et al.*, 2018; Arora and Dash, 2019; Chacko, 2019). The recent cyclone Amphan was derived from the word 'Um-pun', connotation sky, which was

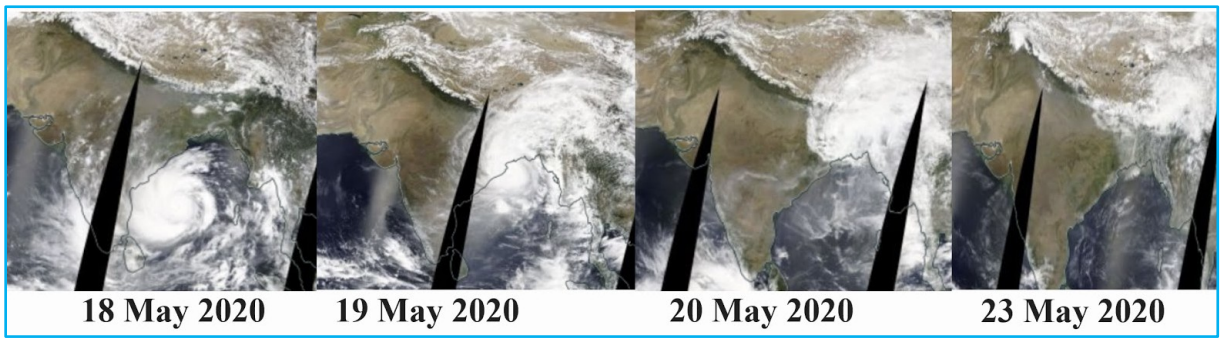

Fig. 1. Satellite image showing movements of Amphan cyclone during 18-23 May 2020

suggested by Thailand in 2004. India, Bangladesh, Myanmar, Pakistan, Maldives, Oman, Sri Lanka and Thailand submit a list of cyclone names from time to time and these countries decide the names from the pool (Mitra *et al*., 2020).

Satellite images from MODIS (Moderate Resolution Imaging Spectroradiometer) (Fig. 1) show movement of Amphan cyclone after formation in the Bay of Bengal to the northward (during 18-23 May, 2020), after the landfall the cyclone moved over the eastern part of India. The movement of the cyclone Amphan was accompanied by strong winds and heavy precipitation which covered the areas of Odisha, West Bengal, Bangladesh and Assam. As the cyclone moved, heavy precipitation occurred causing flood in the areas along the track of the cyclone.

The tropical cyclone Amphan made its landfall at Bakkhali in West Bengal, India at 0230 PM (local time) with wind velocity more than 175 km/h. This cyclone was formed on 16 May, 2020 (0530 IST) and within 12 hours transformed into a deep depression with a maximum sustained (3-min average) wind speed of 56 km/h (Das *et al.*, 2020). The 'eye' of the storm initially shifted generally in N 32° W direction till 17 May, 2020 (1730 IST) and thereafter started to move towards N 24° E and was positioned around 665 km east of Chennai as an extremely severe cyclonic storm on 18 May, 2020 (0230 IST). Subsequently, the system headed N 22° W and strengthened into a super cyclonic storm on 18 May, 2020 at 1130 IST with a sustained wind speed of 222 km/h. The sustained wind speed reached a maximum of 241 km/h on the same day (2330 IST). Afterward, the Amphan continued its movements towards the north and even moved over Assam crossing over Bangladesh.

After landfall of cyclone on 20 May, 2020 in the coastal region of West Bengal, India, the intensity of the cyclone started reducing as it reached close to the ground. Coastal areas of West Bengal, Odisha, and Bangladesh

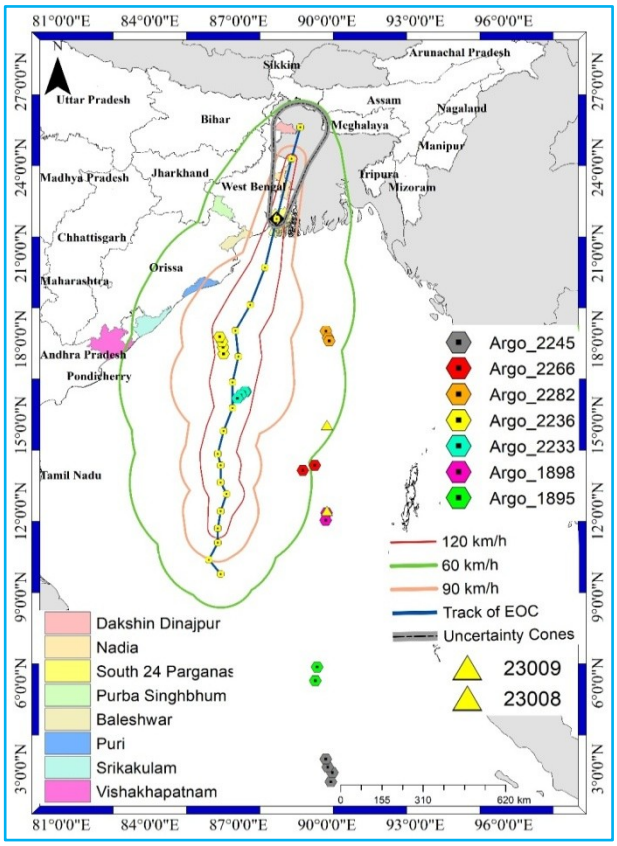

Fig. 2. Showing the track of cyclone along with the location of Argo stations (Color Hexagons), Buoy Sensors (Yellow triangles) and the colored regions in map show the coastal districts of India, used to study the rainfall using Indian Meteorological (IMD) data. (Source of cyclone track : https://www.gdacs.org/resources.aspx?eventid=1000667&episodeid=18&eventtype=TC)

were highly affected by the cyclone. However, the timely forecast of its intensity and regular track of the cyclone helped the different agencies of the government for their preparedness and rescue which drastically brought the lower level of loss of life and property.

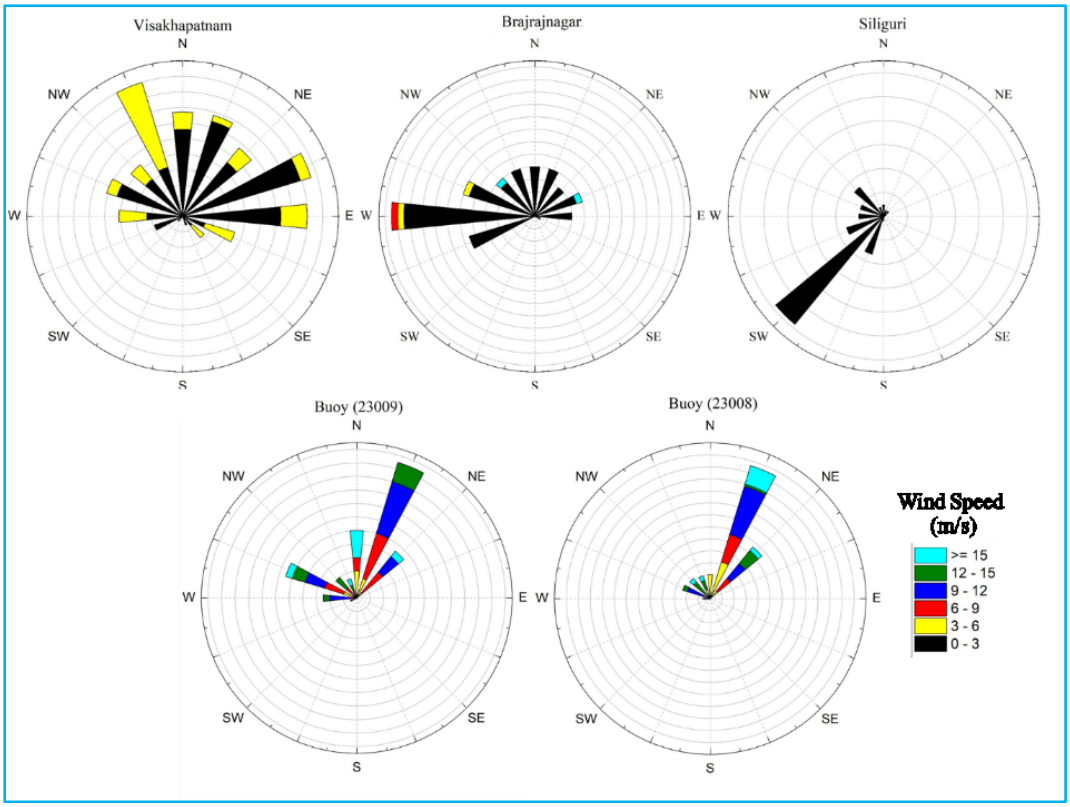

Fig. 3. Average wind Rose diagram during 16-23 May, 2020 over three CPCB stations (Vishakhapatnam - Andhra Pradesh, Brajrajnagar - Odisha state, Siliguri - West Bengal, for coordinates, see Table 1) and two Buoys Stations (Station Id : 23009 and 23008, for coordinates, see Table 3)

The cyclone intensified and moved over Bangladesh coastal areas on 21 May, 2020 as a super cyclone "Amphan" when many of the countries including India and Bangladesh were suffering from COVID-19 pandemic. Due to lockdown, the recovery from cyclone damage was severely affected (Majumdar and Dasgupta, 2020). Even after the cyclone landfall, the wind speed was about 260 km/h. further moved north-east over the Assam causing extreme rainfall and flooding. This cyclone damaged more than 22,000 houses in coastal areas of West Bengal and nearly 220,000 houses in the coastal areas of Bangladesh, affecting approximately 4.2 million people in both countries. This cyclone affected the eastern states of India (Odisha, West Bengal and Assam) and 9 coastal districts of Bangladesh. Heavy rainfall occurred along the track of cyclone, caused intense floods, Kolkata airport was heavily flooded and intense damaged occur, all the domestic and international flights were stopped.

The track of cyclone shown in Fig. 2 is drawn using the GIS platform, we have also shown the location of Argo stations (Colored Hexagons), Buoy (Yellow triangles). The location of the coastal regions is also shown. The intense clouds seen in Fig. 1 brought heavy rainfall along the track of the cyclone.

Fig. 3 shows average wind rose diagram for the periods 16-23 May, 2020 at Vishakhapatnam with varying wind directions NNW - E, at Brajrajnagar - Odisha wind direction is mainly westerly with wind speed up to 6 m/s. The wind direction at Siliguri shows dominant south-westerly wind up to 3 m/s wind speed. The wind data is taken from web (https://cpcb.nic.in/). The surface winds from two Buoys Stations (Station id: 23009 and 23008, coordinates of these Buoys are given in Table 3 (National Data Buoy Center - noaa.gov) which show dominant wind direction (NNE) with the wind speed up to 15 m/s. The surface wind over the sea surface is very high compared to the land stations during the cyclone movements towards land.

The Amphan cyclone caused widespread damage in many parts of different states of India and part of Bangladesh along the track of the cyclone. Fig. 4 shows publicly available photos showing damages caused by heavy rainfall, uprooting of trees, damage to Kolkata airport, electric poles and houses. The intensity of the

Fig. 4. Damages caused by the Amphan cyclone due to high wind speed and rainfall that affected a large population during 16-23 May, 2020

cyclone decreased just before its landfall. The rescue operation was a major challenge due to COVID-19 spread. Amphan cyclone was a deadly cyclone that affected coastal areas and inland areas. The cyclone moved up to Assam after the landfall and heavy rainfall occurred. Along the track of the cyclone, the areas were flooded affecting a large population in the West Bengal, Bangladesh and Assam. The life was standstill for few days due to damage of roads and infrastructure.

3. Data used

In current analysis, we have used the ground data, satellite data and ocean data using difference sources.

3.1. *Satellite data*

We have used the Surface Temperature and Carbon Monoxide Volume Mixing Ratio (CO VMR) data observed by Atmospheric Infrared Sounder (AIRS) satellite. AIRS satellite observed the vertical profile of various meteorological parameters and trace gases at different pressure level during daytime (ascending mode) and nighttime (descending mode).

We have also used the Ozone Monitoring Instrument (OMI) data. OMI is a part of NASA A-train satellite and observed the atmospheric aerosols properties. This satellite also provides information of the total concentration of various atmospheric gases such as NO_2, SO_2 and Ozone. The analysis of total Ozone column is carried out using OMI data with spatial resolution of 0.25° × 0.25° and temporal resolution of 1 day. The data is obtained by NASA Giovanni portal (https://giovanni.gsfc. nasa.gov/giovanni/).

3.2. *Rainfall data*

In current study, we have used NASA Global Precipitation Measurement (GPM) product for the study of rainfall. The integrated Multi-Satellite Retrievals for GPM (IMERG) is a U.S, algorithm that provides the multi satellite precipitation product across the Globe. Version 6 is latest version data that is used here and the details are given at webpage https://disc.gsfc.nasa.gov/datasets/GPM_3IMERGDF_06/summary. We have obtained this by NASA Giovanni portal (https://giovanni.gsfc.nasa.gov/giovanni/) and the spatial resolution of data is 0.1° × 0.1°. We have also used the Indian Meteorological Department (IMD) rainfall data of coastal districts and the districts lies in the direct path of the cyclone. The location of these districts is shown in the Fig. 2.

3.4. *Argo data*

Analysis of Argo floats 2902064 and 2902245 were carried out to study temporal changes of dissolved oxygen (DO), temperature, salinity and chlorophyll concentration for few days in the month of May 2020 when the cyclone Amphan was formed and moved northward over the Bay of Bengal. The vertical depth profile of various parameters from 5 m depth up to 2000 m depth are analyzed at different Argo locations during the movement of cyclone. The Argo floats have 5 days of temporal resolution and are equipped with DO sensors with the accuracy of the factory calibration ~5% or 8 µm for the optode. These sensors were calibrated between 0% and 120% saturation (D'Asaro and McNeil, 2013). There are two quality control levels for the Argo floats data. The real-time automatic quality check is applied initially and later in the second stage a delayed mode quality control systems

TABLE 1

Coordinate of CPCS stations

Station Name	Coordinates
Vishakhapatnam	N - 17.71, E - 83.30
Brajrajnagar	N - 21.80, E - 83.83
Siliguri	N - 26.72, E - 88.39

are used (Thierry and Bittig, 2018). Some details of Argo floats are given recently by Chauhan *et al.* (2021). These data were collected and made freely available by the International Argo Program and the national programs. (http://www. argo.ucsd.edu, http://argo.jcommops.org). The Argo Program is a part of the Global Ocean Observing System. We have considered five Argo float stations (the last four digits of the Argo float Id is shown), coordinates of float locations are given in Table 3.

3.4. *Wind data*

The wind analysis of various locations in India is carried out the Central Pollution Control Board data. We have analyzed the wind at Vishakhapatnam, Brajrajnagar and Siliguri station. The coordinated of these stations are given in Table 1 and the data is available at https://app.cpcbccr.com/ccr/#/caaqm-dashboard-all/caaqm-landing.

In current study, we have also used the Buoy data for the wind analysis in Bay of Bengal. The Buoy data network is known as Ocean Data Acquisition System (ODAS) and it is transmitted hourly through the geostationary satellite to the Global Telecommunication System. This network is distributed throughout the world for ocean data collection for various atmospheric and meteorological analysis. These data were collected and made freely available by NOAA/NDBC (https://www.ndbc.noaa.gov/).

3.5. *GPS (Global Positioning System) Water vapour data*

Water vapour is one of the very important atmospheric parameters, highly variable atmospheric constituent. The efficient transfer of the energy in the atmosphere is transferred depending upon the concentrations of the water vapour in the atmosphere and is one of the important parameters in the formation and propagation of weather. The variability of water vapour in the atmosphere is used as an input parameter in weather forecasting and monsoon forecast (Singh *et al*., 2004). Kumar *et al*. (2009, 2013) have studied variability of water vapour and its relations with rainfall over India.

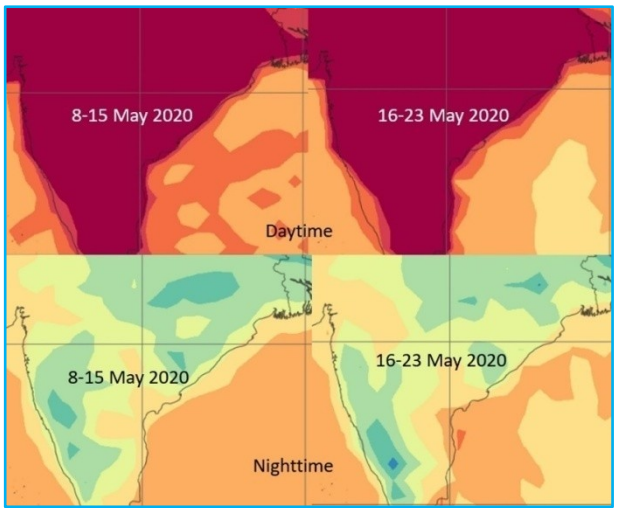

Fig. 5. The surface temperature during daytime and nighttime for the periods 8-15 May, 2020 and 16-23 May, 2020

Prasad and Singh (2009) have carried out detailed analysis of water vapour derived with MODIS, AERONET and GPS data over Indian region and have found very good correlation. Water vapour over Indian region is one of the most poorly characterized meteorological parameters. GPS is deployed at the Indian Institute of Science, Bangalore (Lat. 13.0343, Long. 77.5115) campus as of 13 March, 2000 as a part of the permanent station. The details of water vapour data derived from GPS global stations are discussed in detail by Ware *et al*. (2000). The water vapour retrieved from GPS station is very reliable and this can be used for the forecast of precipitation associated with the cyclone formation in the BoB and its movements. Sarkar *et al*. (2018) have studied variability of water vapour at the Gulf of Mexico associated with the 2017 hurricane Harvey.

4. Results and discussion

4.1. *Surface temperature*

Fig. 5 shows spatial variations of surface temperature(version AIRS AIRS3STD v006) considered through NASA Giovanni portal (https://disc.gsfc.nasa.gov/) of the location during daytime and nighttime for the periods 8-15 May, 2020 (prior to the cyclone formation) and 16-23 May, 2020 (during cyclone movements). Contrast changes in surface temperature over the Bay of Bengal for two periods during daytime and nighttime have clearly been observed. The temperature varies in the range of 20-25 °C. During the daytime, temperature contrast over land and Bay of Bengal is higher compared to nighttime. Pronounced changes in the sea surface temperature during the day and nighttime were observed before 8-15 May and 16-23 May, 2020.

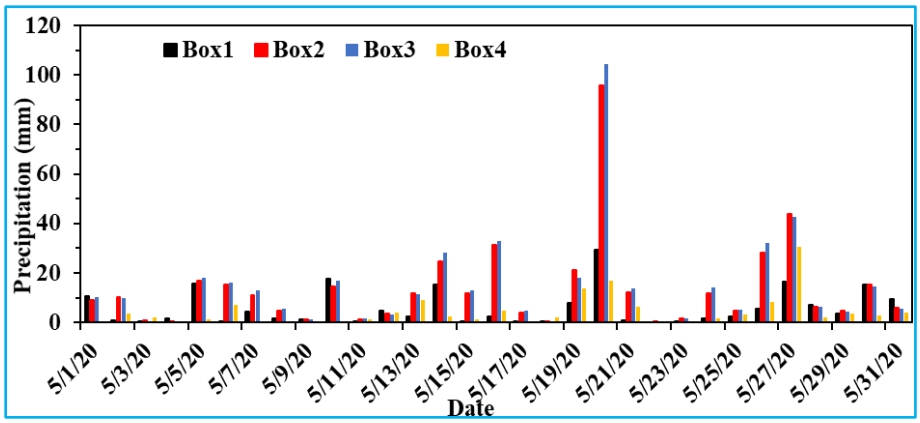

Fig. 6. Daily accumulated precipitation (combined microwave-IR) estimates with resolution 0.1° × 0.1° (precipitation product GPM GPM_3IMERGDE v06) for May 2020 over four boxes)

4.2 *Precipitation*

Fig. 6 shows daily accumulated precipitation (combined microwave-IR) estimate with resolution 0.1 deg. (precipitation productGPM_3IMERGDE v06) for the month of May 2020, the month in which Amphan cyclone was formed. The accumulated precipitation is considered over four boxes; the coordinates of four bounding boxes are given in Table 2. The maximum precipitation occurred on 20 May, 2020. The highest precipitation observed over Box 2 followed over Box 3. The accumulated precipitation of about 50 mm is also seen after a week on 27 May, 2020 over Boxes 2 and 3. The accumulated precipitation increased in Box 3 compared to Box 2, depending upon numerous parameters, such as surface, atmosphere, elevation, heating process and cloud microphysical parameters. The varying accumulated precipitation over these boxes is associated with flooding of different areas in the eastern parts of Indian regions. The heavy precipitation along the track of the cyclone flooded part of areas in West Bengal, Bangladesh and Assam. The strong wind and heavy rainfall were observed as Amphan Cyclone pass over Bangladesh. In Bengal delta, mangrove forest was damaged due to strong wind and heavy precipitation causing flood which was also observed by Hassan *et al.* (2020).

In Fig. 7(a), we have shown the temporal variation of rainfall (mm/day) during 13 May, 2020 to 25 May, 2020. As the cyclone moved from south to north, the rainfall at each location increased. Puri observed the highest amount of rainfall during this time where 396.1mm of rainfall is observed on 20 May, 2020. The southern districts of West Bengal, India, observed more than 100mm of rainfall as per Indian Meteorological Department during this time. Further, in eastern side of West Bengal, more than 80mm/day of rainfall has been observed. These data show

TABLE 2

Coordinate of 4 bounding boxes

Regions	Coordinates of the Bounding box (west, south, east, north) in degree
Box 1	84.4, 22.5, 88.4, 25.5
Box 2	88.4, 22.5, 92.4, 25.5
Box 3	92.4, 22.57, 96.4, 25.5
Box 4	96.4, 22.5, 100.4, 25.5

good correlation with the GPM datasets, the maximum rainfall was observed on 20 May, 2020 (Fig. 6). The variability observed in rainfall over different coastal locations and over four boxes are associated (Figs. 6&7) with the dynamics of cyclone.

Fig. 7(b) shows water vapour derived from GPS observations and surface pressure at the Indian Institute of Science, Bangalore GPS station for the month of May 2020. The GPS derived water vapour shows high values and low surface pressure correspond to the formation of Amphan cyclone in the Bay of Bengal (BoB). As the cyclone in the BoB moves northward, the surface pressure increase. Variations of water vapour and surface pressure show dynamic nature corresponding to the formation of cyclone and its movement. The high water vapour up to more than 40 mm is observed on 138 Julian day (16 May. 2020) followed by low surface pressure. The high water vapour corresponds to high rainfall (more than 60 mm) observed at the Visakhapatnam on 17 May, 2020. As the cyclone moved northward the heavy rainfall in coastal areas were observed [Fig. 7(a)].

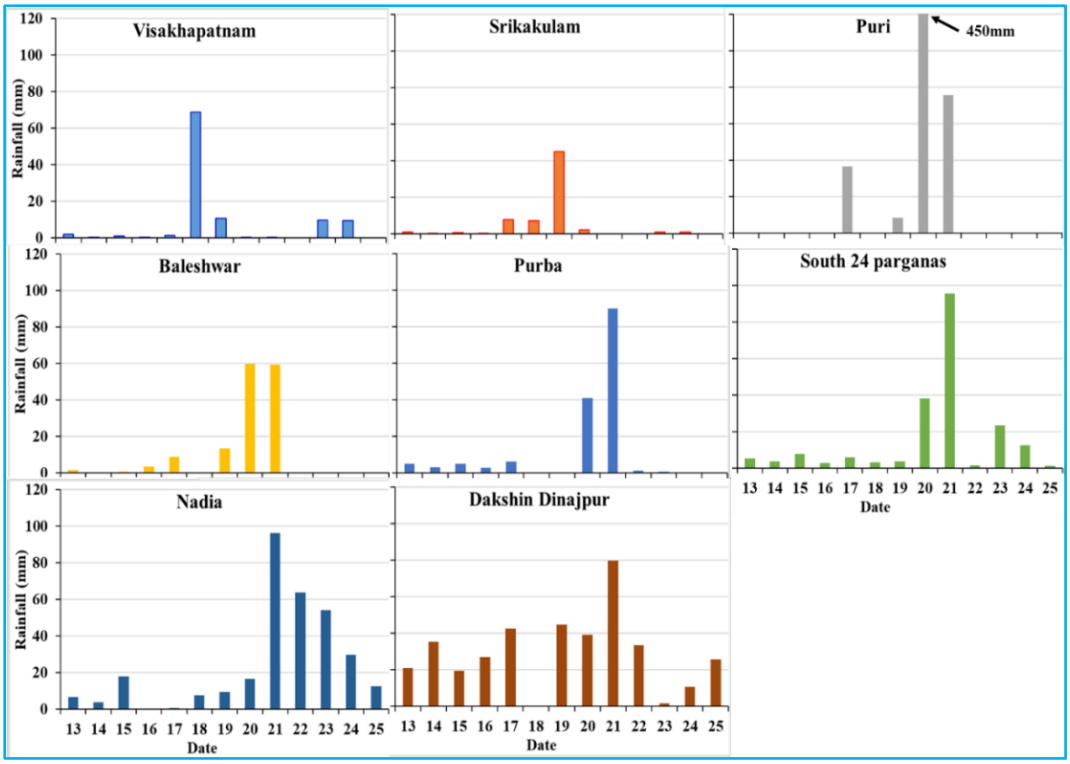

Fig. 7(a). Rainfall in coastal districts of India and districts in direct path of cyclone during 13-25 May, 2020 (*Source of Data* : https://indiawris.gov.in/)

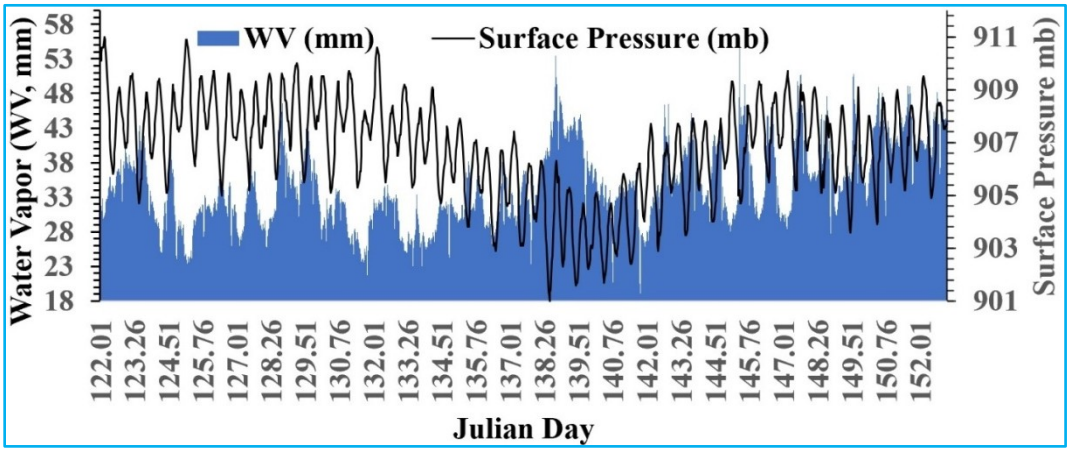

Fig. 7(b). Shows variations of GPS derived water vapour and surface pressure measured at the permanent GPS station for the Julian day of the month of May 2020

Fig. 8 shows the spatial precipitation image using a combined microwave - IR estimate (GPM 3IMERGDF v06) for the month of May 2020. The precipitation data is overlaid on a Google Earth image. Spatial variability of precipitation is seen over the Bay of Bengal for the month of May 2020 along the south-north direction which shows coincidence of the track of Amphan. The red color shows maximum precipitation where the cyclone was formed and moving towards the north. The white color is the lowest region precipitation region and yellow covered areas are lower precipitation areas after the red color region. The precipitation is observed along the track up to Himalayan foothills covering West Bengal, Bangladesh and parts of Assam. Fig. 6 shows temporal variations of precipitation over four boxes.

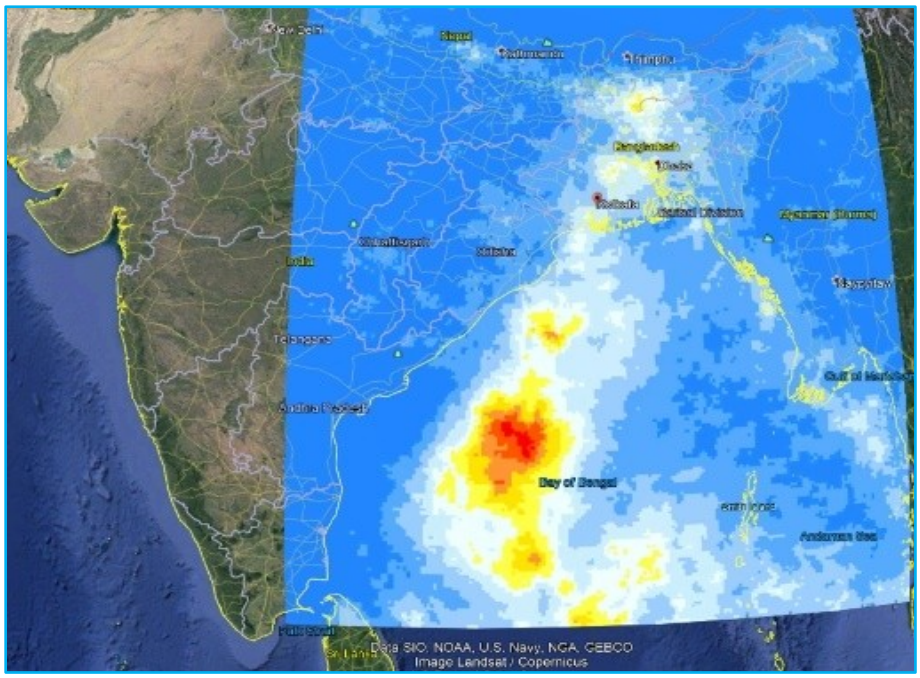

Fig. 8. Spatial precipitation variations through combined microwave – IR estimate (GPM 3IMERGDF v06) for the month of May 2020. The precipitation data is overlaid on a Google Earth image

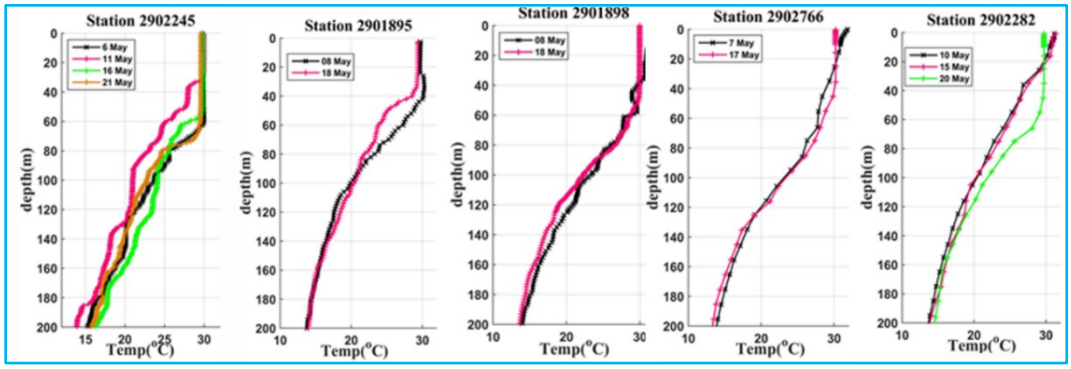

Fig. 9(a). The vertical profile of temperature at different Argo floats locations from south to north, locations of Argo floats are shown in Table 3

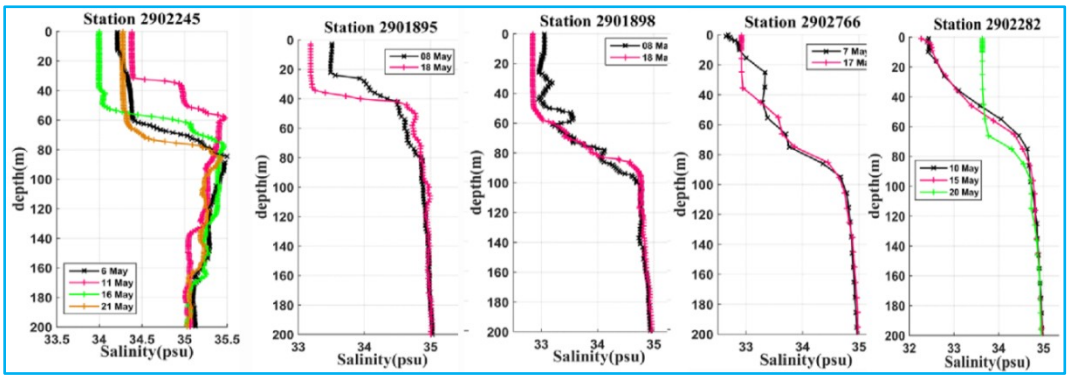

Fig. 9(b). The vertical profile of salinity (psu) at different Argo floats locations from south to north and locations of Argo floats are shown in Table 3

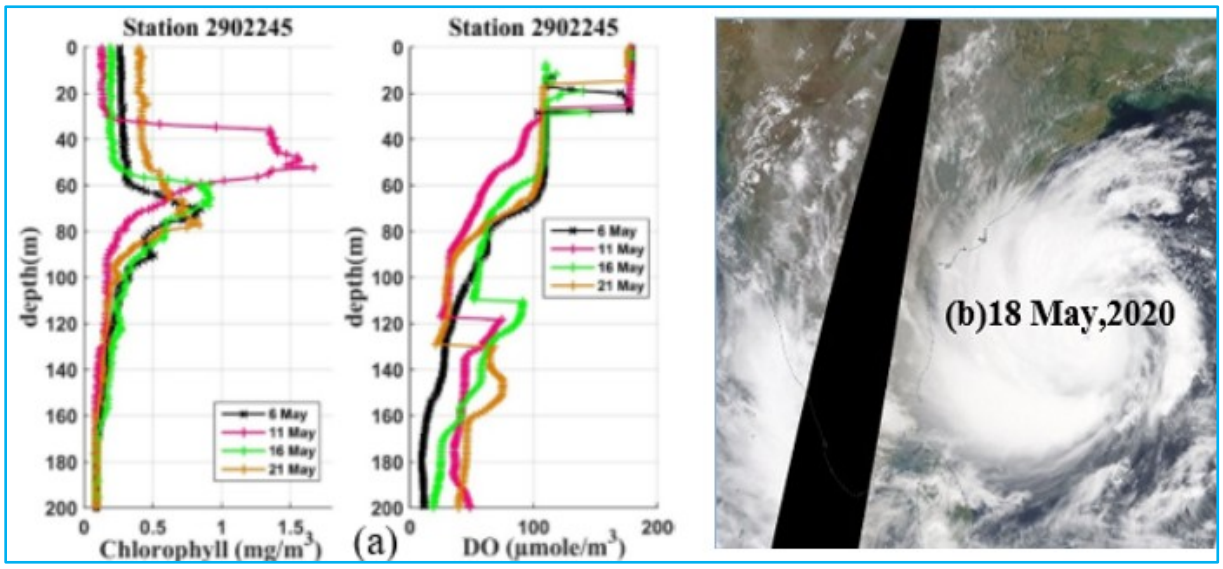

Figs. 10(a&b). (a) Depth profiles of Chlorophyll Concentration and Dissolved Oxygen (DO) at Argo station 2902245 during May 2020 and (b) MODIS image and shows cyclone passes close to southern coast on 18 May, 2020

4.3. *Change in ocean parameters*

We have carried out the analysis of ocean temperature, salinity, Chlorophyll concentration and Dissolved Oxygen (DO) using Argo data from 5m depth to 2000 m at the Argo locations (Fig. 2). The Argo float at the extreme south location (Station 290245) shows a constant temperature up to 40 m, on 11 May, 2020 the temperature sharply decreases [Fig. 9(a)]. The upper surface temperature seems to be constant around 30 °C. A slight change in temperature gradient is seen.

The Argo float (Table 3) is located in the south of the Bay of Bengal, the sea surface temperature on the top is almost the same and the temperature at the depth of 200 m is same at other locations. However, the movement of cyclone along the track in the Bay of Bengal seems to have strong mixing showing a sharp decrease in temperature gradient and the upper layer shows a strong mixing towards Bengal delta. The vertical profile of salinity observed by Argo stations (Table 3) along south to north along the track is shown in Fig. 9(b). As the cyclone moves towards north close to Bengal Delta, strong mixing of ocean water is seen, showing sharp reduction in salinity. Coastal areas of west Bengal and Bangladesh were flooded due to heavy rainfall that is likely to enhance surface runoff of fresh water that may have reduce salinity of upper surface. Fig. 10 shows vertical profile of the chlorophyll concentration and dissolved oxygen (DO) measured by the Argo station 2902245 (for coordinates, see Table 3). Higher chlorophyll concentrations were observed on 11 May, 2020 due to small atmospheric disturbance which is observed from MODIS image on 12 May, 2020 (11 May Modis image is not available). The Argo station (Id 2902245) was affected by the Amphan cyclone as a result the chlorophyll concentration is observed to be higher at the depth 60-80 m compared to 8 and 21 May, 2020. The maximum chlorophyll concentrations were seen at the depth 60-80 m. The vertical profile of dissolved oxygen (DO) observed by the Argo (Id 2902245) is found to be higher at the depth 200-130 m compared to other dates. DO concentration enhanced on 16 May, 2020 as the ocean water was disturbed due to the formation of Amphan cyclone, afterwards DO concentrations decreased.

TABLE 3

Coordinates of Argo floats and Buoys

Argo Id (last four digits)	Lat. (°N)	Long. (°E)
Argo_2245	2.55	90.13
Argo_1895	6.56	89.67
Argo_1898	11.93	89.99
Argo_2766	13.42	89.18
Argo_2233	16.17	87.25
Argo_2236	17.48	86.50
Argo_2282	18.29	89.97
Buoy_23008	12	90
Buoy_23009	15	90

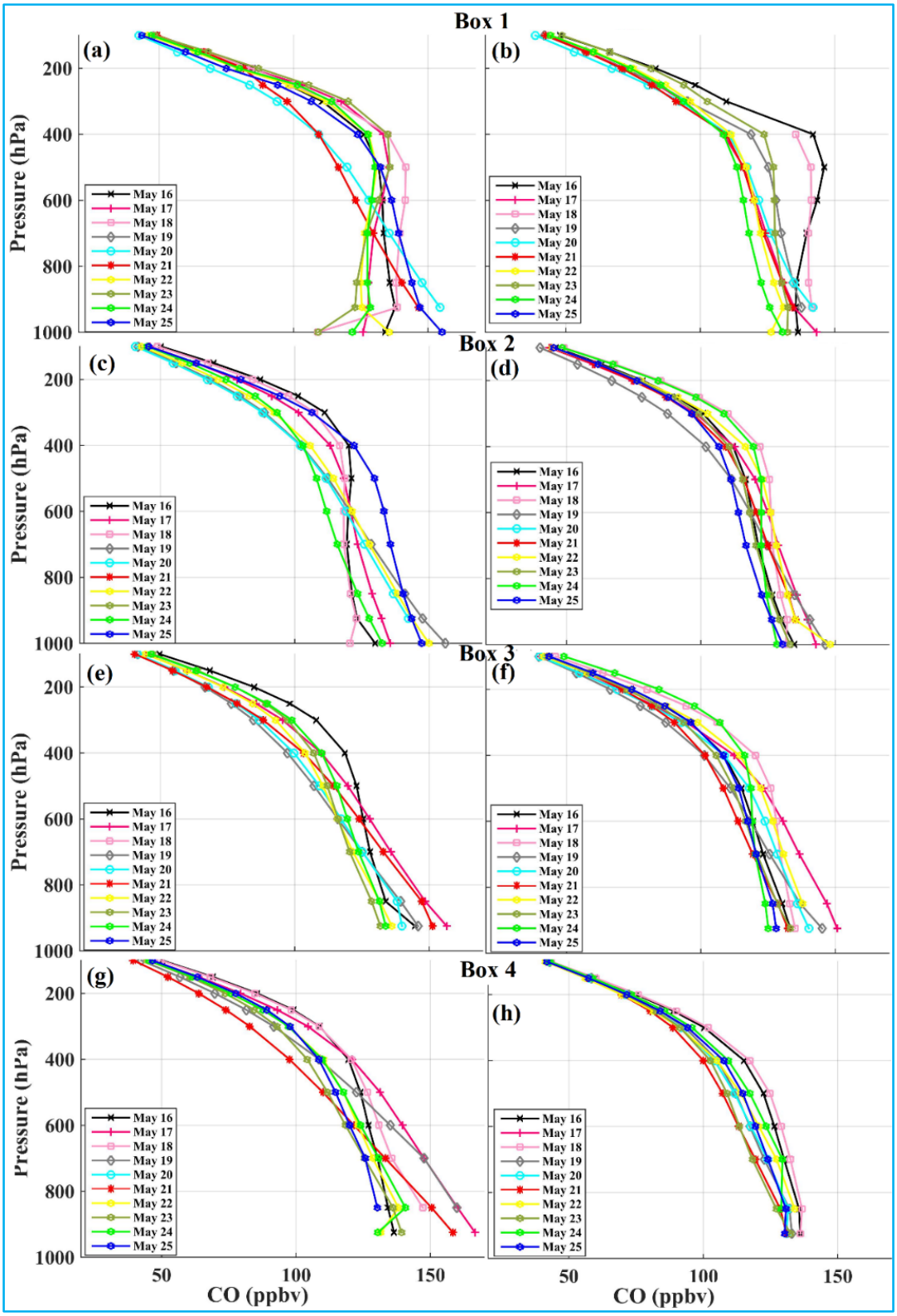

Figs. 11(a-h). Vertical profile of CO VMR over four boxes. The figures in the left panel show the daytime vertical profile and the right panel figures show nighttime vertical profile

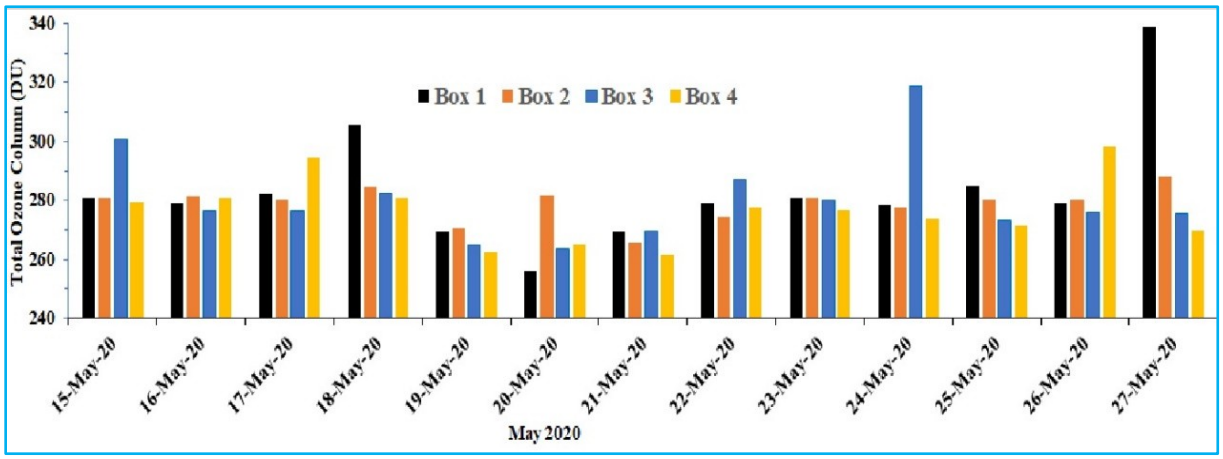

Fig. 12. Variation of total ozone column (TOC) over four boxes (Table 2) during 15-27 May, 2020. Decline in TOC is clearly observed due to landfall of cyclone and with the movement on land after the landfall. Decline in TOC is related to changes in meteorological parameters

Similar results are also observed by Chauhan *et al*. (2021) in the case of Cyclone Fani. The mild storm observed on 12 May, 2020 (MODIS image of 12 May 2020) which corresponds to the changes in DO concentration at a depth of 120 m compared to 16 May, 2020 associated with the Amphan cyclone [Fig. 10(b)].

4.4. *Effect on trace gases*

In Fig. 11, we have shown vertical profile of CO volume mixing ratio over four boxes, Box 1 - 4. The daytime and nighttime profile is shown separately. The cyclonic conditions influence the CO mass concentration in the atmosphere and this effect is shown in Boxes 1, 2 and 3. No major changes are observed in the Box 4. In Box 1, we found that the CO mass concentration increased in the middle troposphere just before the cyclone during day and nighttime. As the cyclone reaches close over the Box 1, sudden rise in CO concentration is observed, close to ground on 20 and 21 May, 2020. Afterwards decline in CO concentration is observed at lower troposphere. The highest CO concentration was found on 20 May, 2020. In Box 2, enhancement in CO concentration is observed on 19 and 22 May, 2020 close to the ground during daytime. In Boxes 3 and 4, the enhancement in CO is observed on 20 and 21 May, 2020 in total vertical column with respect to the concentration prior to the landfall of the cyclone. The CO concentrations over Box 3 and 4 is not pronounced since the track of the cyclone is not close to these locations.

The strong convection associated with cyclone enhances the CO concentration especially close to the ground. Also, we observed an increase in CO concentration in the middle troposphere prior to the landfall of the cyclone. The changes in CO concentrations are associated with the movement of airmass and strong mixing of the anthropogenic emissions locally or from neighboring areas associated with the strong cyclonic wind. The changes in CO concentrations were also observed at the time of dust event (Bhattacharjee *et al.*, 2007; Chauhan *et al*., 2019, 2021).

Variations of total ozone column (TOC) (data product OMI OMDOAO3e v003) with 0.25° × 0.25° spatial resolutions over four boxes are shown for the periods 15-27 May, 2020. The data product is taken through NASA Giovanni portal. Fig. 12 clearly shows decrease in TOC value. Such decline in TOC is also observed by many others (Singh and Singh, 2007; Midya *et al*., 2012; Chaudhuri and Dutta, 2014; Chauhan *et al*., 2018) which is likely due to strong exchanges between troposphere-stratosphere (Pathakoti *et al*., 2016) and enhancement of water vapour destroys the TOC. Further, Midya *et al.* (2012) have explained the decline in TOC through chemical and dynamical processes and water molecules in vapour state in the formation of tropical cyclones.

5. Conclusions

The ground, satellite and ARGO data show contrast changes in the ocean surface temperature and rainfall retrieved from satellite data. Contrasting difference in the daytime and nighttime of ocean water and extreme precipitation associated with the movement of Amphan cycle from south to north. The extreme precipitation shows higher precipitation over the Boxes 2 and 3, that caused flood in the West Bengal, Bangladesh and Assam. The vertical depth profile at different Argo locations show changes in the temperature, salinity, chlorophyll concentrations, dissolved oxygen with the depth in the

ocean observed from Argo stations deployed in the Bay of Bengal. The CO mole fraction in the atmosphere varies over the four boxes that corresponds to the movement of cyclone over the land. This contrasting difference in CO mole formation is associated with the strong winds and heavy precipitation that reduces the concentration of CO mole fraction. With the movement of cyclone over the land there is strong exchanges between land-troposphere-stratosphere that decline the total ozone column (TOC) which is consistent with the similar results associated with past cyclone observed by many others. The results based on the ground, buoys, ARGO and satellite data show existence of strong coupling associated with the Amphan cyclone. The present results will be of great help in modelling of cyclonic process and to forecast the extreme rainfall which is the major cause for flood associated with the cyclones in India especially when cyclone is common in the Bay of Bengal.

Acknowledgments

Our thanks to NASA Giovanni and NOAA/NCDC teams for providing satellite and model data. Special thanks to the NASA Panoply team for providing freeware to plot netCDF file with ease. Argo floats data were acquired freely by the International Argo Program (ARGO project: https://argo.ucsd.edu/data/acknowledging-argo/) and thankfully acknowledged. The authors are grateful to India Meteorological Department and Central Pollution Control Board of India for making rainfall and wind data available at different coastal locations. Thanks to the NASA Giovanni team for making NASA data available through the Giovanni portal and the GDACS (Global Disaster Alerting Coordination System) Team for statistical data related to the cyclone. The authors thank UCAR and Suominet group for providing GPS derived water vapour and surface pressure data observed at the Indian Institute of Science Bangalore GPS station. Thanks to the anonymous referee for constructive comments/ suggestions which have helped us to improve earlier version of the manuscript.

The contents and views expressed in this research paper are the views of the authors and do not necessarily reflect the views of their organizations.

References

Arora, K. and Dash, P., 2019, "The Indian Ocean dipole: a missing link between El Niño Modoki and tropical cyclone intensity in the North Indian ocean", *Climate*, **7**, 3 p38.

Bhattacharjee, P. S., Prasad, A. K., Kafatos, M. and Singh, R. P., 2007, "Influence of a dust storm on carbonmonoxide and water vapour over the Indo-Gangetic Plains", *J. Geophys. Res.- Atm*., **112**, D18, Article Number: D18203.

Chacko, N., 2019, "Differential chlorophyll blooms induced by tropical cyclones and their relation to cyclone characteristics and ocean pre-conditions in the Indian Ocean", *J. Earth Syst. Sci*. **128**, p177.

Chaudhuri, S. and Dutta, D., 2014, "Investigation on the Influence of the Column Ozone Anomaly on the Energetics of Tropical Cyclones Over NIO and Related Air-Sea Interaction", *Pure and Applied Geophysics*, **171**, 2519-2531, doi :10.1007/s00024-014-0800-4.

Chauhan, A., Kumar, R. and Singh, R. P., 2018, "Coupling between Land-Ocean-Atmosphere and pronounced changes in atmospheric/meteorological parameters associated with the Hudhud Cyclone of October 2014", *Int. J. Environ. Res. Public Health*, **15**, p2759.

Chauhan, A., Kumar, R., Dash, P. and Singh, R. P., 2019, "Impact of Fani Cyclone of 2019 on Land, Ocean, Atmospheric and Meteorological Parameters", *AGUFM, 2019*, A21V-2713.

Chauhan, A., Singh, R. P., Dash, P. and Kumar, Rajesh, 2021, "Impact of Tropical Cyclone 'Fani' on Land, Ocean, Atmospheric and Meteorological Parameters", *Marine Pollution Bulletin*, **162**, https://doi.org/10.1016/j.marpolbul.2020.111844.

Chittibabu, P., Dube, S. K., Macnabb, J. B., Murty, T. S., Rao, A. D., Mohanty, U. C. and Sinha, P. C., 2004, "Mitigation of flooding and cyclone hazard in Orissa, India", *Natural Hazards*, **31**, 2 455-485.

D'Asaro, E. A. and McNeil, C., 2013, "Calibration and stability of oxygen sensors on autonomous floats", *J. Atmos. Ocean. Technol.*, **30**, 1896-1906.

Das, S., Das, A., Kar, N. S. and Bandyopadhyay, S., 2020, "Cyclone Amphan and its impact on the Lower Deltaic West Bengal: a preliminary assessment using remote sensing sources", *Current Sci.*, **119**, 8, 1246-1249.

Evan, A. T., Kossin, J. P. and Ramanathan, V., 2011, "Arabian Sea tropical cyclones intensified by emissions of black carbon and other aerosols", *Nature*, **479**, 7371, 94-97.

Frank, W. M. and Roundy, P. E., 2006, "The role of tropical waves in tropical cyclogenesis. *Mon. Wea. Rev*.", **134**, 9, 2397-2417.

Gautam, R., Cervone, G., Singh, R. P. and Kafatos, M., 2005a, "Characteristics of meteorological parameters associated with Hurricane Isabel", *Geophys. Res. Lett.*, **32**, L04801.

Gautam, R., Singh, R. P. and Kafatos, M., 2005b, "Changes in ocean properties associated with Hurricane Isabel", *Int. J. Remote Sens.*, **26**, 643-649.

Hassan, M. M., Ash, K., Abedin, J., Paul, B. K. and Southworth, J., 2020, "A Quantitative Framework for Analyzing Spatial Dynamics of Flood Events: A Case Study of Super Cyclone Amphan", *Remote Sens*., **12**, p3454.

Knutson, T. R., McBride, J. L., Chan, J., Emanuel, K., Holland, G., Landsea, C., Held, I., Kossin, J. P., Srivastava, A. K. and Sugi, M., 2010, "Tropical cyclones and climate change", *Nature Geoscience*, **3**, 3, 157-163.

Kumar, Sanjay, Singh, A. K., Prasad, A. K. and Singh, R. P., 2009, "Annual Variability of water vapour from GPS and MODIS data over the Indo-Gangetic Plains", *J. Ind. Geophys. Union*, **13**, 1, 17-23.

Kumar, Sanjay, Singh, A. K., Prasad, A. K. and Singh, R. P., 2013, "Variability of GPS derived water vapour and comparison with MODIS data over the Indo-Gangetic plains", *Phys. and Chemistry of the Earth*, 11-18, doi: 10.1016/j.pce.2010.03.040.

Kundu, S. N., Sahoo, A. K., Mohapatra, S. and Singh, R. P., 2001, "Change analysis using IRS-P4 OCM data after the Orissa super cyclone", *Int. J. Remote Sens.*, **22**, 1383-1389.

Majumdar, B. and Dasgupta, S., 2020, "Let Bengal be heard: dealing with Covid and cyclone Amphan together", *South Asian History and Culture*, **11**, 3, 317-322. doi: 10.1080/ 19472498. 2020.1780063.

Midya, S. K., Dey, S. S. and Chakraborty, B., 2012, "Variation of the total ozone column during tropical cyclones over the Bay of Bengal and the Arabian Sea", *Meteorol. Atmos. Phys.*, **117**, 63-71. doi : 10.1007/s00703-011-0169-1.

Mitra Abhijit, Dutta, J., Mitra, A. and Thakur, T., 2020, "Amphan Super cyclone: A death knell for Indian Sundarbans", *eJournal of Applied Forest Ecology (eJAFE)*, **8**, 1, 41-48.

Mohanty, C. R., Bellapukonda, S., Ahmad, S. R. and Sarkar, S., 2019, "Seconds from disaster-crisis in critical care unit during tropical cycloneFani", *J. Clin. Anesth*, **60**, 72-73.

Mohapatra, M. and Sharma, M., 2019, "Cyclone warning services in India during recent years: A review", *MAUSAM*, **70**, 4, 635-666.

Mohapatra, M., Bandyopadhyay, B. K. and Tyagi, A., 2014, "Construction and Quality of best tracks parameters for study of climate change impact on Tropical Cyclones over the North Indian Ocean during satellite era, in: Monitoring and Prediction of Tropical Cyclones in the Indian Ocean and Climate Change", Springer, 3-17.

Pathakoti, Mahesh, Sujatha, P., Karri, Srinivasa Rao, Sai Krishn, S. V. S. and Rao, P. V. N., 2016, "Evidence of stratosphere-troposphere exchange during severe cyclones : A case study over Bay of Bengal, India", *Geomatics, Nat. Hazards Risk*, **7**, 1816-1823.

Powell, M. D. and Reinhold, T. A., 2007, "Tropical cyclone destructive potential by integrated kinetic energy", *Bulletin of the American Meteorological Society*, **88**, 4, 513-526.

Prasad, A. K. and Singh, R. P., 2009, "Validation of MODIS Terra, AIRS, NCEP/DOE AMIP-II Reanalysis-2 and AERONET Sun photometer derived integrated precipitable water vapour using ground-basedGPS receivers over India", *J. Geophys. Res*., **114**, Article Number: D05107.

Rao, A. D., Upadhaya, P., Ali, H., Pandey, S. and Warrier, V., 2020, "Coastal inundation due to tropical cyclones along the east coast of India : An influence of climate change impact", *Nat. Hazards*, 1-18.

Roman Stork, H. L. and Subrahmanyam, B., 2020, "The Impact of the Madden-Julian Oscillation on Cyclone Amphan (2020) and Southwest Monsoon Onset", *Remote Sens.*, **12**, p3011.

Sarkar, S., Singh, R. P. and Chauhan, A., 2018, "Anomalous changes in meteorological parameters along the track of 2017 Hurricane Harvey", *Remote Sens. Lett.*, **9**, 487-496.

Singh, D. and Singh, V., 2007, "Impact of tropical cyclone on total ozone measured by TOMS-EP over the Indian region", *Curr. Sci*., **93**, 4, 471-476.

Singh, O. P., Masood, T. and Khan, A., 2001, "Rahman, M.S. Has the frequency of intense tropical cyclones increased in the north Indian Ocean?", *Curr. Sci*., **80**, 575-580.

Singh, R. P., 2003, "Early warning of natural hazards using satellite remote sensing", *Curr. Sci.*, **89**, 592-593.

Singh, R. P., Cervone, G., Kafatos, M., Prasad, A. K., Sahoo, A. K., Sun, D., Tang, D. L. and Yang, R., 2007, "Multi-sensor studies of the Sumatra earthquake and tsunami of 26 December, 2004", *Int. J. Remote Sens.*, **28**, 13-14.

Singh, R. P., Dey, S., Sahoo, A. K. and Kafatos, M., 2004, "Retrieval of water vapour using SSNM and its relation with the onset of monsoon", *Annales Geophsicae*, **22**, 8, 3079-3083.

Tang, D. L., Satyanarayana, B., Zhao, H. and Singh, R. P., 2006, "A Preliminary Analysis of the Influence of Sumatran Tsunami on Indian Ocean CHL-A and SST", *Adv. Geosci.*, **5**, 15-20.

Tang, D., Zhao, H., Satyanarayana, B., Zheng, G., Singh, R. P., Lv, J. and Yan, Z., 2009, "Variations of chlorophyll - a in the northeastern Indian Ocean after the 2004 South Asian tsunami", *Int. J. Remote Sens.*, **30**, 4553-4565

Thierry, V. and Bittig, H., 2018, "Argo quality control manual for dissolved oxygen concentration", doi : 10.13155/46542.

Turton, S. M. and Stork, N. E., 2008, "Impacts of tropical cyclones on forests in the Wet Tropics of Australia", In : Living in a Dynamic Tropical Forest Landscape, (eds N. E. Stork & S. M. Turton), Wiley-Blackwell Publishing, Oxford., 47-58.

Ware, R. H., Fulker, D. W., Stein, S. A., Anderson, D. N., Avery, S. K., Clark, R. D., Droegemeier, K., Kuettner, J. P. and Minster, J. B., 2000, "Suominet : A real-time national GPS network for atmospheric research and education", *Bulletin of the American Meteorological Society*, **81**, 677-694.